# Flux penetration measurements and the harmonic magnetic response of hot isostatically pressed (Pb,Gd)$Mo_6S_8$

H. D. Ramsbottom and D. P. Hampshire[a)]
*Department of Physics, University of Durham, Durham, United Kingdom*

(Received 26 October 1998; accepted for publication 23 December 1998)

Detailed flux penetration measurements and the harmonic magnetic response have been measured from 4.2 K up to the critical temperature in dc fields up to 10 T for a hot isostatically pressed Chevrel-phase superconductor (Pb,Gd)$Mo_6S_8$. Good agreement is found between experimental results up to the tenth harmonic and calculations derived from a critical-state model which demonstrates that on the macroscopic scale the supercurrents flow throughout the *bulk* of the material. The field and temperature dependence of the critical current density shows a universal scaling behavior in agreement with Kramer's pinning law, which suggests that a single grain-boundary mechanism determines the critical current density. Complementary compositional microscopy, x-ray, resistivity, and susceptibility data are presented. When gadolinium is not incorporated into the crystal structure it acts primarily as an oxygen getter in the form $Gd_2S_3$, which enhances the density of paths of $PbMo_6S_8$ with low oxygen content and high superconducting critical parameters. When the divalent gadolinium replaces the trivalent lead to form $(Pb_{1-x}Gd_x)Mo_6S_8$, it reduces the density of hole states at the Fermi energy which lowers the critical parameters, the critical current density, and the irreversibility field. © *1999 American Institute of Physics.* [S0021-8979(99)00507-1]

## I. INTRODUCTION

High upper critical field ($\mu_0 H_{C2}$) values of Chevrel-phase (CP) superconductors[1] make them promising candidates for high-field applications.[2,3] Recently significant improvements in the critical current density ($J_C$) and the irreversibility field ($\mu_0 H_{\rm irr}$) of Chevrel-phase wires of composition (Pb,Sn)$Mo_6S_8$ (Ref. 4) have been reported, but for practical magnet construction further increases in $J_C$ by a factor of 2–4 are required.[5] An unusual property of CP material is that it remains superconducting even when rare-earth (RE) ions are incorporated into its structure. Early work on increasing the critical parameters of $PbMo_6S_8$ was successful when gadolinium was added. The Gd caused an increase in the unit cell size of the CP structure together with improvements in the upper critical field ($\mu_0 H_{C2} = 54$ T at 4.2 K) and the critical temperature ($T_C \sim 14$ K).[6] In this article, we present detailed flux penetration measurements made in high magnetic fields and investigate whether Gd can increase the $J_C$ of $PbMo_6S_8$.

The study of the electromagnetic properties of superconductors has been markedly improved by the flux penetration technique first developed by Campbell.[7] These measurements enable nondestructive determination of the spatial variations in the superconducting properties, which facilitates identifying where the supercurrent flows and, hence, regions of high $J_C$. Nevertheless, these measurements are not common because for bulk samples, the measurements require high ac fields, which is a demanding experimental requirement in the presence of high dc fields. This article presents flux penetration and harmonic measurements from 4.2 K up to $T_C$ in dc magnetic fields up to 10 T on material of nominal composition $Pb_{0.7}Gd_{0.3}Mo_6S_8$ [(Pb,Gd)$Mo_6S_8$] hot isostatically pressed (HIPed) at $2\times10^8$ N m$^{-2}$ (2000 bar). A purpose-built probe provides large ac fields of up to 100 mT.[8] Comparison is made between the results and a critical-state model that describes supercurrent flowing throughout the bulk of the material. In contrast to standard dc magnetic measurements[9] or transport measurements,[10] changes in bulk properties can be explicitly distinguished from percolative or surface properties. By measuring the spatial variation of $J_C$ in high magnetic fields nondestructively, the effect of the Gd on the bulk properties of (Pb,Gd)$Mo_6S_8$ is determined.

Flux penetration measurements with small ac fields have found very high $J_C$ values at the surface of $PbMo_6S_8$ samples ($>10^{10}$ A m$^{-2}$ at 5 T and 4.2 K), which demonstrates the potential of this material.[11] However, the short coherence length of $PbMo_6S_8$ can lead to granular properties if the structure or stoichiometry varies on that length scale. Hence, the degree of granularity and the critical superconducting parameters are strongly dependent on the fabrication procedure.[12] In previous work on ternary $PbMo_6S_8$ samples, we found that the irreversibility field can be significantly increased by using hot isostatic pressing (HIPing).[13] All the quaternary samples reported in this work have been HIPed to improve their connectivity.

Section II describes the experimental procedure. This includes details of the sample fabrication together with compositional microscopy, x-ray, resistivity, and susceptibility data. These show that the sample is not single phase and confirm that adding Gd does improve the critical superconducting parameters.[6] The flux penetration and harmonic measurement techniques are also outlined. In Secs. III and IV the

a)Electronic mail: d.p.hampshire@dur.ac.uk

 

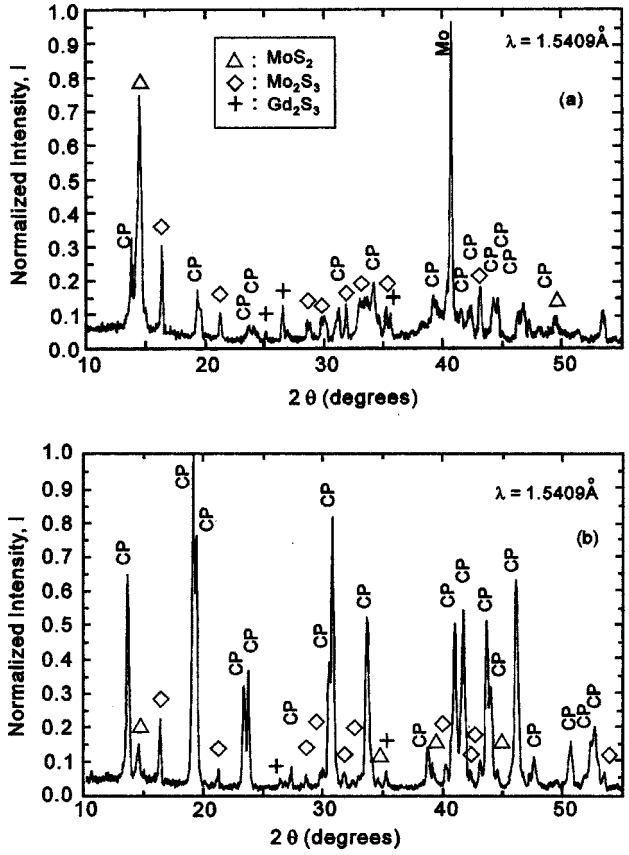


FIG. 1. X-ray diffraction pattern for (Pb,Gd)$Mo_6S_8$: (a) before HIPing; (b) after HIPing; and CP denotes Chevrel-phase structure.

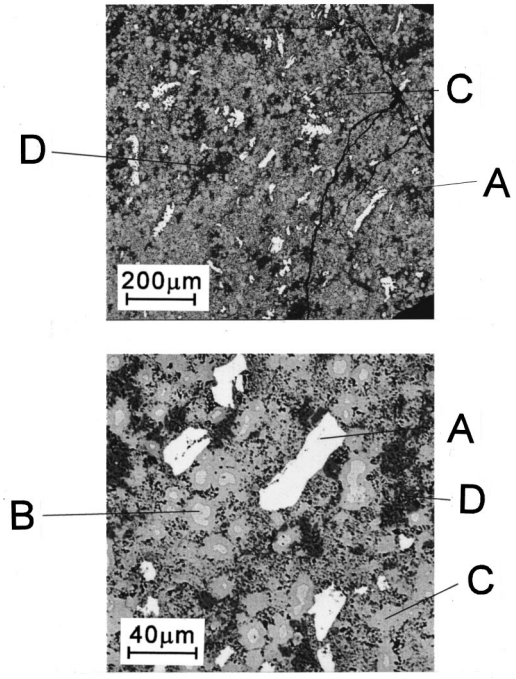


FIG. 2. Electron probe microanalysis HIPed (Pb,Gd)$Mo_6S_8$. The phases labeled are A: $Gd_2S_3$, B: Mo, C: $Pb_{1-x}Gd_xMo_6S_8$, and D: $MoS_2$, $Mo_2S_3$.

results are presented and analyzed. The experimental results have been used to calculate magnetic-field profiles which are then compared to model calculations.[14] $J_C(B,T)$ is presented and analyzed within the framework of a universal scaling law. At the end of the article, there is a discussion of the effect of adding Gd to HIPed polycrystalline $PbMo_6S_8$ samples and a summary of the most important findings.

## II. EXPERIMENT

### A. Sample preparation and quality

The fabrication procedure for the series of samples investigated in this work follows that reported previously.[15] In brief, pure elements were mixed in the nominal composition $(Pb_{1-x}Gd_x)Mo_6S_8$ for $x=0.0$, 0.1, 0.2, and 0.3. The powders were repeatedly ground, pressed, and reacted to form the intermediate sulphides. Then, the material was sealed under vacuum in silica tubes and reacted at 1000 °C for 44 h. Finally, the samples were wrapped in molybdenum, sealed under vacuum in stainless-steel tubes and heat treated in a hot isostatic press (HIP) at $2\times10^8$ N m$^{-2}$ (2000 bar) at 800 °C for 8 h. The sample, which has been measured in detail (i.e., $x=0.3$), has been characterized using x-ray diffraction (XRD) both before and after HIPing, as shown in Fig. 1. HIPing ensures that the dominant phase has the CP structure, with minority phases of $MoS_2$, $Mo_2S_3$, and $Gd_2S_3$. Consistent with these results, $MoS_2$ and $Mo_2S_3$ have been reported at 1000 °C (Refs. 16 and 17) and $Gd_2S_3$ at 1100 °C.[18] Figure 2 shows low magnification electron probe microanalysis (EPMA) results for the HIPed sample, in which the spatial distribution of the different phases present can be seen. Elemental mapping shows that most of the Gd occurs in phase A ($Gd_2S_3$), however, there is a layer about 5–10 $\mu$m thick surrounding phase A which also contains a small amount of Gd. In this layer, the Gd content decreases as the Pb content increases, consistent with Gd-doped $PbMo_6S_8$.[19] Figure 3 shows the irreversibility field (as determined by resistivity measurements using a sample current of ~3 mA) as a function of temperature for samples with different levels of Gd content. Adding a small amount of Gd dramatically increases the critical parameters for the onset of superconductivity. Thereafter, there is no change in the irreversibility field as

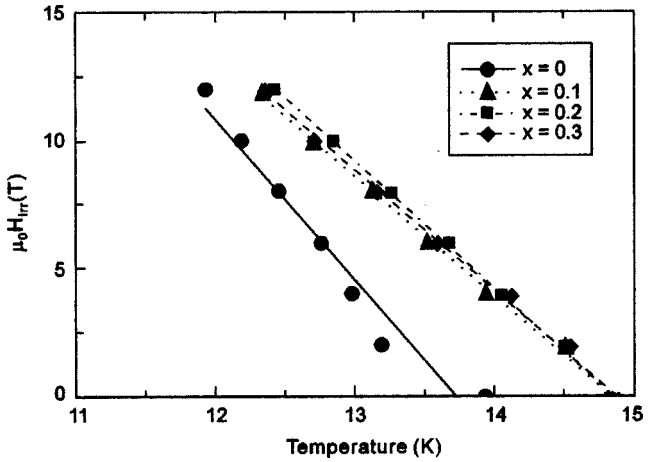


FIG. 3. Irreversibility field as a function of temperature $[\mu_0 H_{irr}(T)]$ for $Pb_{1-x}Gd_xMo_6S_8$ samples of different gadolinium content. $\mu_0 H_{irr}(T)$ is defined by the onset of the resistivity transition.

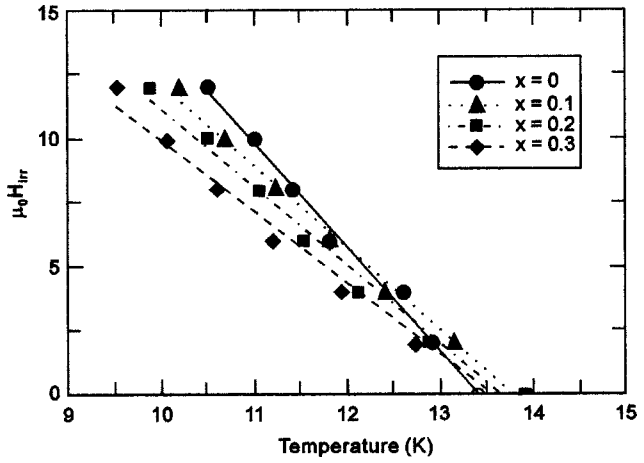


FIG. 4. Irreversibility field as a function of temperature $[\mu_0 H_{\rm irr}(T)]$ for $Pb_{1-x}Gd_xMo_6S_8$ samples of different gadolinium content. $\mu_0 H_{\rm irr}(T)$ is defined by the onset of the susceptibility transition.

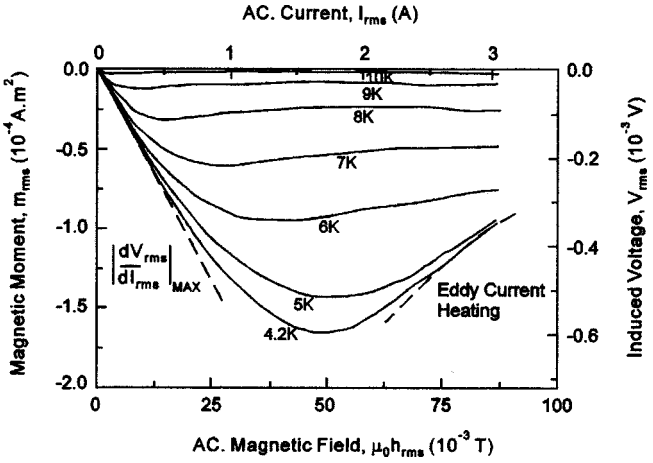


FIG. 5. Magnetic moment vs ac field for HIPed (Pb,Gd)$Mo_6S_8$ as a function of temperature in an axial dc field of 5 T.

the Gd content is increased. In Fig. 4, equivalent data for the irreversibility field as determined from susceptibility measurements (using an ac field of about $10^{-4}$ T) show a quite different trend. Although the temperature for the onset of superconductivity in zero field increases, in high magnetic fields the opposite occurs. The onset of superconductivity is at a lower temperature as more Gd is added to the sample. An explanation for the difference between the irreversibility field determined from the resistivity and susceptibility data is discussed in Sec. V.

### B. Flux penetration measurements

The (Pb,Gd)$Mo_6S_8$ sample was cut into dimensions 1.0 mm×1.0 mm×5.0 mm. A purpose-built probe[8] was used to make flux penetration measurements from 4.2 K up to $T_C$ in a dc field up to 10 T. In these measurements, the sample experiences an ac field of up to 100 mT at 19.7 Hz (produced by the superconducting primary coil of the probe) superimposed on a large dc field (produced by the superconducting magnet). The direction of the ac field is parallel to the dc field. The magnetic response of the sample is monitored by measuring the induced voltage across two secondary coils of similar geometry, wound in opposite sense. Measurements were performed with the magnetic fields applied both parallel (axial) and perpendicular (transverse) to the long axis of the sample.

## III. RESULTS

Figure 5 shows the magnetic moment ($m_{\rm rms}$) versus ac field ($\mu_0 h_{\rm rms}$) for the (Pb,Gd)$Mo_6S_8$ as a function of temperature in an axial field of 5 T. The current through the primary coil of the probe and the induced voltage across the secondary coils are also included. The rms ac current is converted to the ac field using the primary coil constant ($C$) of 28.7 mT $A^{-1}$. The induced voltage is converted into a rms magnetic moment using the secondary coils calibration constant ($P$) at 19.7 Hz of 0.277 A $m^2$ $V^{-1}$. A background signal, taken when the temperature is above the critical temperature ($T_C$) has been subtracted from all data. At all temperatures, there is a sharp fall in the magnetic moment to a minimum value after which there is a slow increase as the ac field is increased beyond that required for full penetration. The marked increase at high ac fields (at 4.2 and 5 K) is attributed to eddy current heating in the copper components of the probe. Figure 6 shows the magnetic moment versus ac field for the sample in the axial orientation as a function of dc field at 7 K. The maximum ac field which can be obtained at high temperatures and high dc fields is determined by the superconducting primary coil quenching. Figures 7 and 8 show the harmonic response of both the lossless (i.e., the induced voltage 90° out of phase with the current in the primary coil) and the loss (i.e., the induced voltage in phase with the current in the primary coil) components of the induced voltage for (Pb,Gd)$Mo_6S_8$ at 6 K and 3 T. Measurements have been made from 1 F, which is the (fundamental) frequency of the applied ac field, up to 10 F. The even harmonics (which are zero for both components, i.e., less than $\pm 5$ $\mu$V) and the odd harmonics have the functional form expected for bulk supercurrent flow, as discussed in Sec. IV.

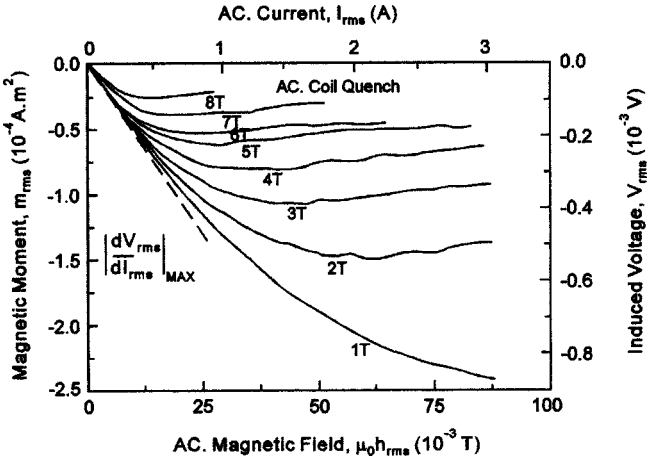


FIG. 6. Magnetic moment vs ac field for HIPed (Pb,Gd)$Mo_6S_8$ as a function of axial dc field at 7 K.

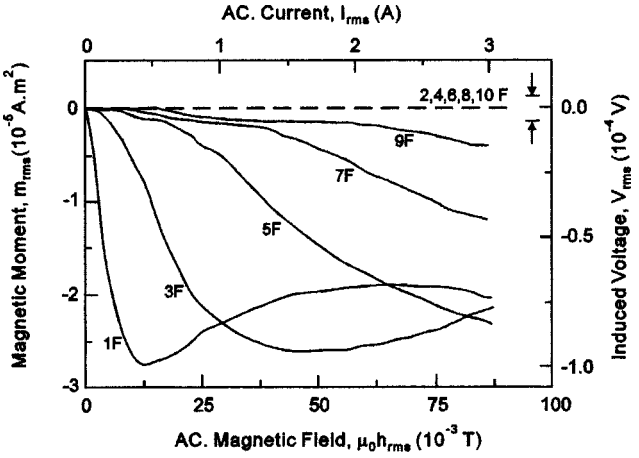


FIG. 7. Harmonic response of the lossless component of the induced voltage for HIPed (Pb,Gd)$Mo_6S_8$ at 6 K in an axial dc field of 3 T.

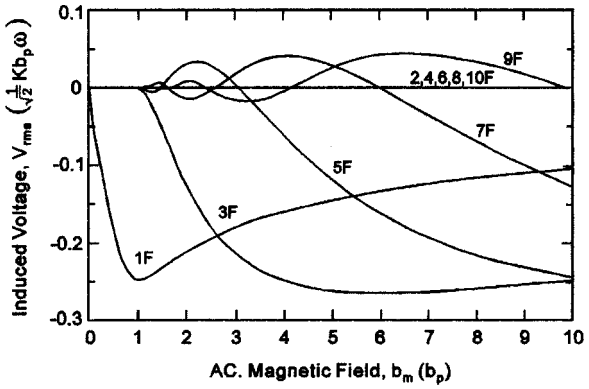


FIG. 9. Calculated lossless component of the induced voltage as a function of axial ac field. $K$ is a constant determined by the shape of the sample and the calibration constant for the secondary coils. $b_p$ is the dc field required to fully penetrate the sample. $\omega$ is the angular frequency of the applied ac file and $b_m$ the peak value during the cycle.

A complete set of data including the field, temperature, and harmonic response has also been obtained for the sample in the transverse orientation.

## IV. ANALYSIS OF RESULTS

### A. Flux profiles

Calculations have been performed of the ac magnetic response of a bulk superconductor to low-frequency, high-amplitude, ac magnetic fields in flux penetration measurements.[14] In the analysis it was assumed that as the ac field increases, the instantaneous flux profile obeys the critical-state model.[20] Solutions have been found for both transverse and axial orientations of cylindrical samples. A Fourier analysis was used to determine the harmonic response at multiple frequencies of the ac field (1 F) up to 10 F. Figures 9 and 10 show the lossless and loss components of the induced voltage as a function of ac field for different frequencies. In these figures all of the even harmonics are zero. For the lossless component (Fig. 9), the magnitudes of the minima in the 1 and 3 F signals are similar, and the field at which these minima occur are about a factor of 4 apart. For the loss component (Fig. 10), the 1 F signal increases monotonically. There is a factor of approximately 2.5 between the ac field required to produce a minimum signal for the 3 and 5 F signals. The experimental data shown in Figs. 7 and 8 follow these predictions very closely, which provides strong evidence that the magnetic response in (Pb,Gd)$Mo_6S_8$ is consistent with the flow of supercurrent throughout the bulk of the material.

Using the data in Figs. 5 and 6, it is possible to determine explicitly the magnetic-field profiles inside the (Pb,Gd)$Mo_6S_8$ sample and, hence, the spatial variation in $J_C$.[8,15] Figures 11 and 12 show the calculated spatial variation in the magnetic field ($\mu_0 M$) inside the (Pb,Gd)$Mo_6S_8$ sample. The distance the field has penetrated ($\delta$) can be approximated by

$$\delta = r_m \left( 1 - \frac{|dV_{\rm rms}/dI_{\rm rms}|}{|dV_{\rm rms}/dI_{\rm rms}|_{\rm max}} \right), \tag{1}$$

where $r_m$ is given by

$$r_m = \left( \frac{\mu_0 P}{\pi L C} \left| \frac{dV_{\rm rms}}{dI_{\rm rms}} \right|_{\rm max} \right)^{1/2}. \tag{2}$$

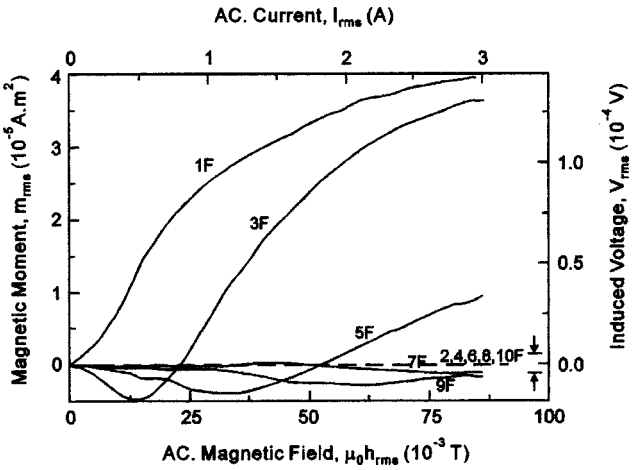


FIG. 8. Harmonic response of the loss component of the induced voltage for HIPed (Pb,Gd)$Mo_6S_8$ at 6 K in an axial dc field of 3 T.

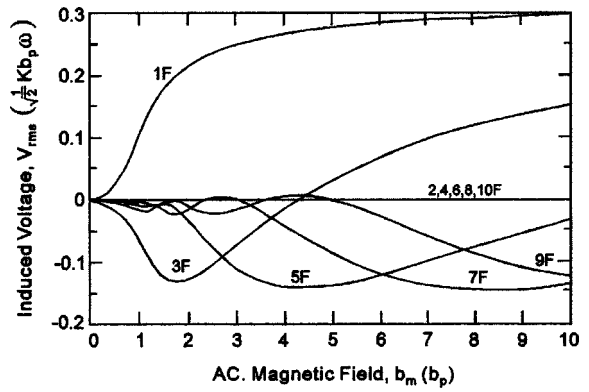


FIG. 10. The calculated loss component of the induced voltage as a function of axial ac field. $K$ is a constant determined by the shape of the sample and the calibration constant for the secondary coils. $b_p$ is the dc field required to fully penetrate the sample. $\omega$ is the angular frequency of the applied ac field and $b_m$ the peak value during the cycle.

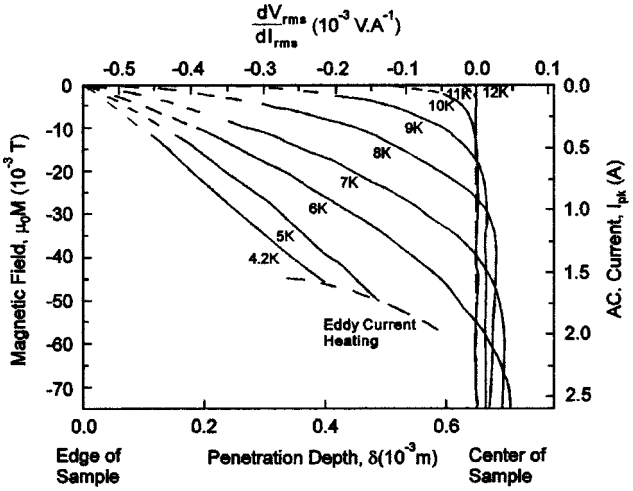


FIG. 11. Magnetic-field profile inside HIPed (Pb,Gd)$Mo_6S_8$ as a function of temperature in axial dc field of 5 T.

$P=0.277\ \mathrm{A\,m^2\,V^{-1}}$, $C=28.7\ \mathrm{mT\,A^{-1}}$, and the length of the sample $L=5$ mm. The derivative $dV_{\mathrm{rms}}/dI_{\mathrm{rms}}$ has been calculated using the Savitsky–Golay method of simplified least squares.[21] The magnetic field inside the sample ($\mu_0 M$) is calculated from

$$\mu_0 M = C I_{\mathrm{pk}}, \tag{3}$$

where $I_{\mathrm{pk}}$ is the peak value of the current in the primary coil during a cycle. The gradient of the field profile as a function of the penetration depth in Figs. 11 and 12 gives the spatial variation of $J_C$. The gradients are rather constant throughout most of the sample as is expected for a bulk pinning superconductor. The minimum in the magnetic moment in Figs. 5 and 6 leads to an apparent penetration of the magnetic field to a depth greater than the radius of the sample. This has been interpreted as evidence for granularity,[22] but detailed calculations demonstrate that this overshot is an artifact of the harmonic analysis.[14]

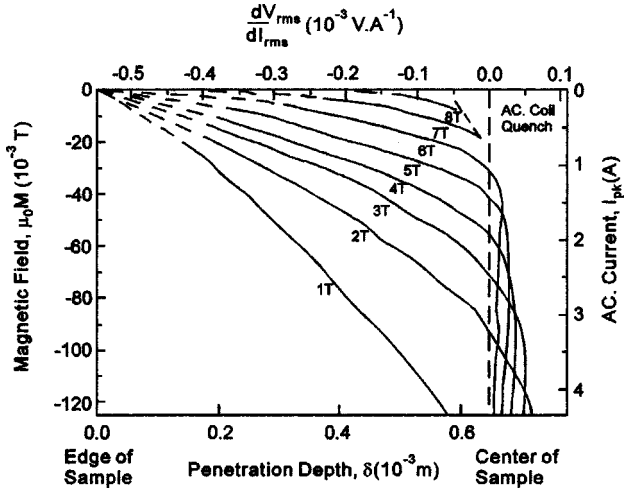


FIG. 12. Magnetic-field profile inside HIPed (Pb,Gd)$Mo_6S_8$ as a function of axial dc field at 7 K.

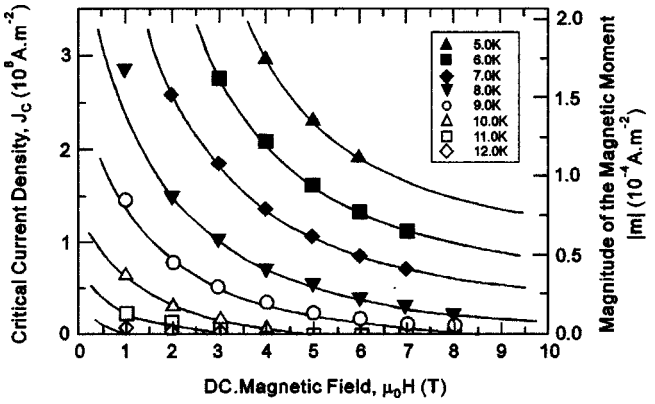


FIG. 13. Critical current density of HIPed (Pb,Gd)$Mo_6S_8$ as a function of field and temperature.

### B. Critical current density and scaling

$J_C$ can be calculated from the minimum rms value of the magnetic moment [$m_{\mathrm{rms}}(\mathrm{min})$] at each field and temperature.[13] In particular,

$$J_C(B,T) = \frac{4.42\ m_{\mathrm{rms}}(\mathrm{min})}{Vr}, \tag{4}$$

where $V$ is the volume of the cylinder and $r$ is its radius. In Fig. 13, the $J_C$ values calculated from the data obtained in axial orientation are presented for the (Pb,Gd)$Mo_6S_8$ sample. The values of $J_C$ are accurate to about 10%, primarily due to the uncertainty in the sample dimensions. At 5 T and 6 K, $J_C$ is $1.6\times10^8\ \mathrm{A\,m^{-2}}$. This is approximately half that for the undoped $PbMo_6S_8$, which gives a value of $3.0\times10^8\ \mathrm{A\,m^{-2}}$.[13] When the appropriate demagnetization factor has been included for the transverse data, the $J_C(B,T)$ graphs are very similar for both orientations.

Figure 14 shows Kramer plots[23] for the (Pb,Gd)$Mo_6S_8$ sample. A linear extrapolation of the data to $J_C^{1/2}(\mu_0 H)^{1/4}=0$ gives the irreversibility field ($\mu_0 H_{\mathrm{irr}}$) for each temperature. The volume pinning force is calculated using $F_p=\mu_0(J_C\times H)$. Figure 15 shows the reduced volume pinning force ($F_P/F_{P\mathrm{MAX}}$) versus the reduced magnetic field ($h=H/H_{\mathrm{irr}}$) for temperatures from 5 to 11 K. As seen by other

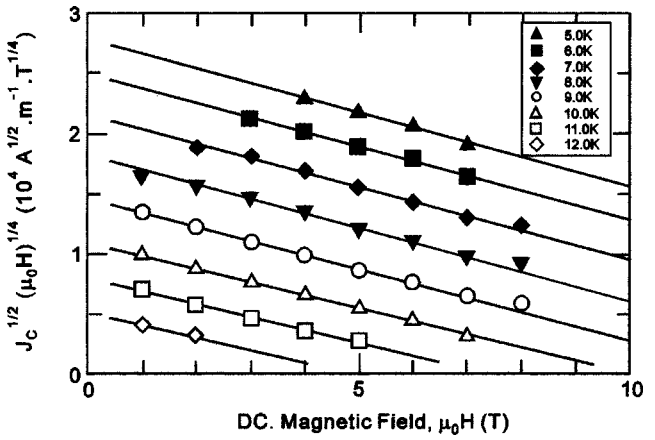


FIG. 14. Kramer plot for HIPed (Pb,Gd)$Mo_6S_8$ as a function of field and temperature.

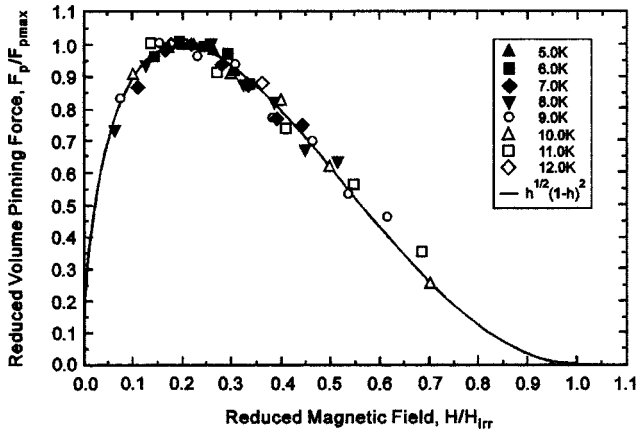


FIG. 15. Reduced volume pinning force vs reduced magnetic field for HIPed (Pb,Gd)$Mo_6S_8$ as a function of temperature showing a universal scaling behavior.

authors, the volume pinning force obeys a universal scaling law of the form $F_P=\alpha(\mu_0 H_{\rm irr})^n h^{1/2}(1-h)^2$, where the constant $\alpha=(1.95\pm0.15)\times10^5$ T$^{-1.79}$ A m$^{-2}$ and the index $n=2.79\pm0.13$.

Figure 16 shows the irreversibility field for (Pb,Gd)$Mo_6S_8$ plotted as a function of temperature. The irreversibility field has been calculated for the data obtained in both axial and transverse orientation and is compared to that for an undoped sample. The solid squares show values of the upper critical field for undoped $PbMo_6S_8$ obtained by dc magnetization measurements.[15]

## V. DISCUSSION

The role of the Gd has been investigated in detail by making flux penetration measurements (Figs. 7 and 8) and measuring the harmonic response (Figs. 11 and 12) of $PbMo_6S_8$, and comparing these data with a critical-state model. Very good agreement is found between experiment and calculations in both axial and transverse field orientations. We conclude that the supercurrent flows throughout the bulk of the (Pb,Gd)$Mo_6S_8$ on the macroscopic scale

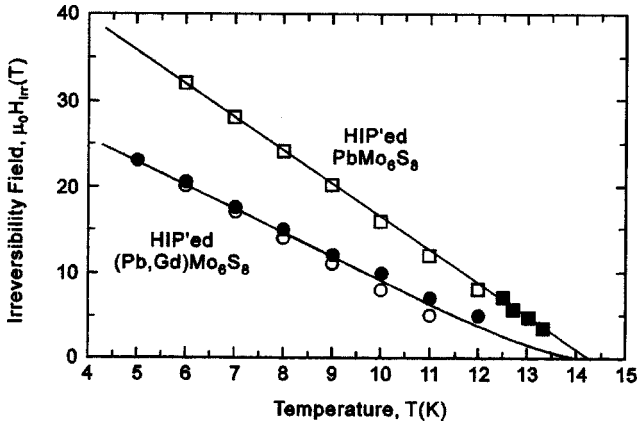


FIG. 16. Irreversibility field for HIPed (Pb,Gd)$Mo_6S_8$ as a function of temperature compared to that for an undoped sample (□). Flux penetration measurements were made with the sample in an axial (●) and a transverse orientation (○). Also shown are values of $\mu_0 H_{C2}$ for $PbMo_6S_8$ (■) from dc magnetization measurements (see Ref. 9).

rather than, for example, preferentially at the surface. The calculations have been completed assuming that $J_C$ does not change significantly when the ac field is applied. From Fig. 13, it is clear that the change in $J_C$, as the ac field is increased up to ≤100 mT, is typically less than 3%, which can be neglected. However, very close to the upper critical field where $J_C$ drops to zero or close to zero field where $J_C$ is a strong function of field, more complex calculations that explicitly include the field dependence of $J_C$ and, hence, include changes in $J_C$ caused by applying the ac field are required.[24,25]

On the microscopic scale, the XRD and microprobe data demonstrate that the sample is multiphase with both the CP compounds $GdMo_6S_8$ and $PbMo_6S_8$ present along with several others including $Gd_2S_3$. The difference in the irreversibility field determined from the resistivity and the susceptibility measurements can be explained by the inhomogeneity of the samples. A marked feature of the resistivity data is the saturation in the irreversibility field. When Gd is first added to the material (cf. Fig. 3), the irreversibility field increases, but further increases in Gd content produce little additional change. The current density flowing during the resistivity measurement is relatively small ($\sim10^3$ A m$^{-2}$) and the voltage generated high so the occurrence of a percolative superconducting current path is all that is required at this characteristic irreversibility field. Since resistivity measurements characterize the percolative paths with the highest critical parameters, and it is known both that the Gd can act as an oxygen getter in the form of $Gd_2S_3$,[26] and that low oxygen content can improve $PbMo_6S_8$,[27,28] we conclude that the Gd enhances the density of low oxygen content $PbMo_6S_8$ paths with very high critical parameters. The irreversibility fields determined from the susceptibility measurements are similar to the irreversibility fields determined from the Kramer extrapolations. When the sample screens out the $10^{-4}$ T ac field, applied during the susceptibility measurements, a current density of about $10^5$ A m$^{-2}$ is flowing. Necessarily, the similarity in the irreversibility field from the susceptibility measurements and the Kramer extrapolation occurs since in both measurements it characterizes the field at which the critical current density has dropped to about $10^5$ A m$^{-2}$. In conclusion, the very marked difference between the irreversibility field determined from the resistive measurements and the susceptibility measurements occurs because of the different criteria used in each case. In the resistive case the irreversibility field is characteristic of percolative superconductivity, whereas for the susceptibility measurement the irreversibility field occurs when the critical current density is about $10^5$ A m$^{-2}$ and is characteristic of the bulk.

The field and temperature dependence of $J_C$ is consistent with a Kramer's flux pinning universal scaling law. Very clear scaling has been observed, which is generally taken a evidence that a single grain-boundary mechanism determines $J_C$.[29] In the original work by Kramer,[23] it was suggested that unpinned fluxons in the grains sheared past fluxons pinned at grain boundaries. More recent work[30] suggest that grain boundaries are channels of very weak flux pinning so that phase coherence and tunneling at the grain boundaries are the important features of the mechanism. At present there is

no general agreement on how the grain-boundary mechanism, which leads to the Kramer dependence, operates. Nevertheless, adding Gd has significantly reduced both $J_C$ and $\mu_0 H_{\rm irr}$ by approximately 50%. By measuring the irreversibility field using flux penetration measurements, this reduction is unambiguously associated with a reduction in bulk properties rather than percolative properties.

The CP superconductors have attracted a great deal of interest because a magnetic RE ion can be incorporated in the crystal structure without destroying the superconductivity. Evidence for the coexistence of magnetic order and superconductivity was first obtained from specific heat and ac susceptibility measurements.[31,32] The most important aspect of the chemical structure is the strongly bonded $Mo_6S_8$ octahedra where the superconductivity is expected to reside. As with rhodium borides, nickel–boron carbides and the high-temperature superconductors, the RE ions are relatively isolated from the superelectrons.[33,34] The trivalent Gd substitutes onto the divalent lead sites in CP superconductors and affects the critical parameters primarily through a charge transfer to the $Mo_6S_8$.[1] The monotonic reduction in the irreversibility field and the high-field susceptibility data suggest that adding the magnetic element Gd is almost entirely detrimental to the high-field properties. Although it is reasonable to assume the degradation in superconductivity occurs both at the grain boundaries and the grains, it is not possible from these measurements to associate the degradation with any specific location in the material at the micron sale. This rules out distinguishing any difference between the grains and the grain boundaries. Recently, $J_C$ data for $(Pb,Gd)Mo_6S_8$ fabricated at 1500 °C have been reported. For this much higher fabrication temperature, the Gd is more uniformly distributed throughout the material and the critical parameters measured both using resistivity and susceptibility decrease monotonically.[35] This demonstrates that incorporating the Gd into the CP structure reduces the superconducting critical parameters of the grains.

We conclude that the Gd affects the properties of $PbMo_6S_8$ in two ways. First, it acts as an oxygen getter in the form of $Gd_2S_3$, which enhances the density of low oxygen content $PbMo_6S_8$ paths with very high critical parameters.[7,28] This is the dominant effect when the material is fabricated at ~1000 °C. Second, it degrades the fundamental superconducting properties when it is incorporated into the CP structure by a charge-transfer mechanism which lowers the density of hole states at the Feri energy. This effect dominates when the material is fabricated at ~1500 °C. In the HIPed $(Pb,Gd)Mo_6S_8$ materials presented here, both mechanisms operate.

## VI. CONCLUSION

A hot isostatically pressed Chevrel-phase superconductor of nominal composition $(Pb_{0.7},Gd_{0.3})Mo_6S_8$ has been measured using flux penetration measurements. The field and temperature dependence of the critical current density show universal scaling in agreement with Kramer's flux shearing model. This scaling suggests that a single grain-boundary mechanism determines the critical current density. Adding gadolinium decreases the critical current density and the irreversibility field by about 50%.

Results from flux penetration measurements have been compared to a critical-state model which described the functional form of the magnetic response of a superconducting sample in an applied ac magnetic field. Measurements have been completed for a cylindrical sample in both axial and transverse orientation up to the tenth harmonic of the ac field. The experimental flux profiles and harmonic response of $(Pb,Gd)Mo_6S_8$ show very good agreement with calculations that demonstrate the supercurrent flows throughout the *bulk* of the material.

In these samples, the gadolinium is an oxygen getter in the form of $Gd_2S_3$ which enhances the density of low oxygen content $PbMo_6S_8$ paths with very high critical parameters. It also degrades the fundamental superconducting properties when incorporated in the Chevrel-phase structure by a charge-transfer mechanism which reduces the density of hole states at the Fermi energy. No preferential degradation has been found at the grains or the grain boundaries. In HIPed material, adding Gd results in a net reduction in $\mu_0 H_{\rm irr}$ and $J_C$ at high magnetic fields.

## ACKNOWLEDGMENTS

The authors wish to thank Professor M. Goringe and Dr. C. Eastell for supplying the microprobe data, Dr. H. Hamid, Dr. D.-N. Zheng, and members of the superconductivity group for useful discussions, Professor J. Howard and Dr. C. W. Lehman for use of the XRD facilities, and P. Russell for help with the production of the figures. This work was supported by the EPSRC and The Royal Society, U.K.

[1] O. Fischer, Appl. Phys. **16**, 1 (1978).
[2] R. Odermatt, O. Fischer, H. Jones, and G. Bongi, J. Phys. C **7**, L13 (1974).
[3] R. Chevrel, M. Hirrien, and M. Sergent, Polyhedron **5**, 87 (1987).
[4] N. Cheggour, M. DeCroux, O. Fischer, and D. P. Hampshire, J. Appl. Phys. (to be published).
[5] B. Seeber, C. Rossel, and O. Fischer, in *Ternary Superconductors*, edited by G. K. Shenoy, B. D. Dunlap, and F. Y. Fradlin (Elsevier, North-Holland, Amsterdam, 1981), p. 261.
[6] O. Fischer, H. Jones, G. Bongi, M. Sergent, and R. Chevrel, J. Phys. C **7**, L450 (1974).
[7] A. M. Campbell, J. Phys. C **2**, 1492 (1969).
[8] H. D. Ramsbottom and D. P. Hampshire, Meas. Sci. Technol. **6**, 1349 (1995).
[9] D. N. Zheng, S. Ali, H. A. Hamid, C. Eastell, M. Goringe, and D. P. Hampshire, Physica C **291**, 49 (1997).
[10] H. A. Hamid, Ph.D. thesis, University of Durham, U.K. (1997).
[11] T. Matsushita, K. Kajiyama, K. Yamafuji, K. Hamasaki, and T. Komata, Jpn. J. Appl. Phys., Part 1 **25**, 831 (1986).
[12] H. Yamasaki, M. Umeda, S. Kosaka, Y. Kimura, T. C. Willis, and D. C. Larbalestier, J. Appl. Phys. **70**, 1606 (1991).
[13] H. D. Ramsbottom and D. P. Hampshire, Physica C **274**, 295 (1997).
[14] H. D. Ramsbottom and D. P. Hampshire, J. Phys.: Condens. Matter **9**, 4437 (1997).
[15] D. N. Zheng, H. D. Ramsbottom, and D. P. Hampshire, Phys. Rev. B **52**, 1 (1995).
[16] S. Yamamoto, M. Wakihara, and M. Taniguchi, Mater. Res. Bull. **20**, 1493 (1985).
[17] H. Yamasaki and Y. Kimura, Mater. Res. Bull. **21**, 125 (1986).
[18] A. W. Sleight and C. T. Prewitt, Inorg. Chem. **7**, 2282 (1986).
[19] C. Eastell, Ph.D. thesis, University of Oxford, U.K. (1998).
[20] C. P. Bean, Rev. Mod. Phys. **36**, 31 (1964).
[21] A. Savitsky and M. J. E. Golay, Anal. Chem. **36**, 1627 (1964).

[22] F. Gomory, S. Takacs, P. Lobotka, K. Frohlich, and V. Plechacek, Physica C **160**, 1 (1989).
[23] E. J. Kramer, J. Appl. Phys. **44**, 1360 (1977).
[24] J. R. Clem, J. Appl. Phys. **50**, 3518 (1979)
[25] J. D. Thompson, M. P. Maley, and J. R. Clem, J. Appl. Phys. **50**, 3531 (1979).
[26] D. G. Hinks, J. D. Jorgensen, and H. Li, Solid State Commun. **49**, 51 (1984).
[27] D. W. Capone II, P. R. Guertin, S. Foner, D. G. Hinks, and H. C. Li, Phys. Rev. B **29**, 6375 (1984).
[28] S. Foner, E. J. McNiff, Jr., and D. G. Hinks, Phys. Rev. B **31**, 6108 (1985).
[29] M. O. Rikel, T. G. Togonidze, and V. I. Tsebro, Sov. Phys. Solid State **28**, 1496 (1986).
[30] D. P. Hampshire, Physica C **296**, 153 (1998).
[31] R. W. McCallum, D. C. Johnson, R. N. Shelton, and M. B. Maple, Solid State Commun. **29**, 391 (1977).
[32] R. W. McCallum, D. C. Johnson, R. N. Shelton, W. A. Fertig, and M. B. Maple, Solid State Commun. **24**, 501 (1977).
[33] *Superconductivity in Ternary Compounds*, edited by S. O. Fischer and M. B. Maple (Springer, Berlin, 1982).
[34] R. J. Cava, H. Takagi, H. W. Zandbergen, J. J. Kajewski, W. F. Peck, T. Siegrsit, B. Batlogg, R. B. van Dover, R. J. Felder, K. Mizuhashi, J. O. Lee, H. Eisaki, and S. Uchida, Nature (London) **367**, 252 (1994).
[35] D. N. Zheng, A. B. Sneary, and D. P. Hampshire, in *Proc. EUCAS 1997* [Inst. Phys. Conf. Ser. **158**, 1005 (1997)].